Available online at www.sciencedirect.com
ScienceDirect
Journal of Magnetism and Magnetic Materials 316 (2007) e883–e885
Journal of magnetism and magnetic materials
www.elsevier.com/locate/jmmm

Magnetic properties of melt-spun FeMnAlB alloys

I. Betancourt[a,*], F. Nava[b]

[a]Departamento de Materiales Metálicos y Cerámicos, Instituto de Investigaciones en Materiales, Universidad Nacional Autónoma de México, Mexico D.F. 04510, Mexico
[b]Instituto Tecnológico de Tlalnepantla, Av.Instituto Tecnologico s/n, Tlalnepantla, Edo de Mexico, 54070, Mexico

Available online 19 March 2007

Abstract

Magnetic properties of melt spun $Fe_{89-x}Mn_{11}Al_x$ ($x = 2, 4, 8, 15$) and $Fe_{87-y}Mn_{11}Al_2By$ ($y = 6, 8, 10$) alloy series were studied by vibrating sample magnetometry and complex permeability measurements. The saturation magnetization exhibited an initial high value of 210 emu/g followed by a decreasing tendency with increasing Al and B additions (up to 139 emu/g). On the other hand, the initial permeability showed variations within the range 1000–2000, whereas the relaxation frequency displayed a maximum of 2 MHz for the 4 at% Al alloy.

PACS: 75; 75.20.En; 75.30.Cr; 75.50.Bb

Keywords: Soft magnetic material; Fe-based alloy; Melt spun alloy

1. Introduction

Disordered Fe–Mn–Al alloys have been a system of interest from both technical and fundamental point of view due to their excellent mechanical properties and their highly sensitive composition-dependence magnetic ordering, which can include ferromagnetic, antiferromagnetic, spin glass or re-entrant spin glass behaviour [1–3]. Most studies focus on bulk alloys with high Mn/Al contents processed by die-casting and further annealing-quenching treatment [1–3]. In this report, we present a study of DC and AC magnetic properties of FeMnAlB metallic ribbons obtained by chill block melt spinning process.

2. Experimental techniques

The alloy series $Fe_{89-x}Mn_{11}Al_x$ ($x = 2, 4, 8, 15$) and $Fe_{87-y}Mn_{11}Al_2B_y$ ($y = 6, 8, 10$) were prepared by using the chill block melt spinning technique with a roll speed of 20 m/s, from master ingots previously obtained by arc-melting commercially grade Fe, Mn, Al, B constituents within inert Ar atmosphere. The alloys microstructure was monitored by X-ray diffraction analysis with Cu-Kα radiation. DC magnetic properties were determined by means of a vibrating sample magnetometer VSM at a maximum field of 5 kOe, whilst complex permeability measurements were carried out on ribbon alloy samples wounded as toroids of 16 mm diameter by using an HP 4192A impedance analyzer with an applied AC field of 10.2 A/m (rms) and a frequency variation within the range 10 Hz–13 MHz. The real and imaginary components of the complex permeability, used for Cole–Cole plots, were determined from the components of the complex impedance according to the complex permeability formalism [4,5].

3. Results

X-ray diffractograms (XRD) for $Fe_{87}Mn_{11}Al_2$, $Fe_{85}Mn_{11}Al_4$ and $Fe_{81}Mn_{11}Al_2B_6$ alloy ribbons are shown in Fig. 1. The (1 1 0), (2 0 0), (2 1 1), (2 2 0) and (3 1 0) α-Fe refraction peaks were identified for all the alloy series. According to Ref. [3], up to 17 at% Al content, only the disordered BCC phase is present in FeMnAl with similar Fe:Mn ratio. For this disordered phase, all sites are occupied with the same probability by Fe, Mn or Al

*Corresponding author. Tel.: +52 55 56224654; fax: +52 55 56161371.
E-mail address: israelb@correo.unam.mx (I. Betancourt).

0304-8853/$ - see front matter © 2007 Elsevier B.V. All rights reserved.
doi:10.1016/j.jmmm.2007.03.128

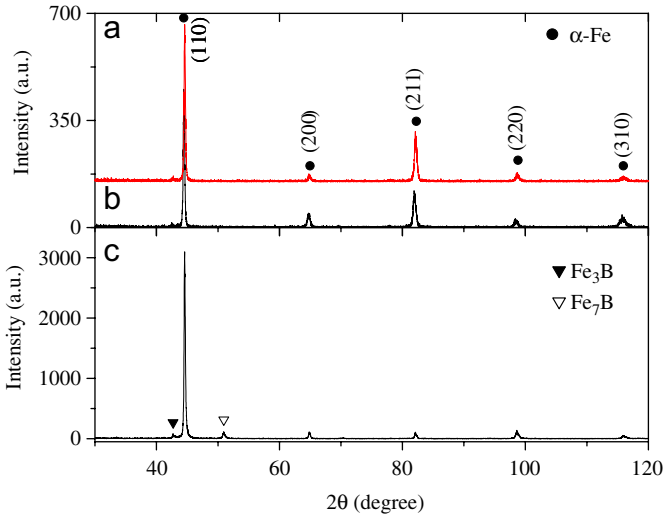

Fig. 1. XRD for (a) $Fe_{87}Mn_{11}Al_2$, (b) $Fe_{85}Mn_{11}Al_4$ and (c) $Fe_{81}Mn_{11}Al_2B_6$ alloy ribbons.

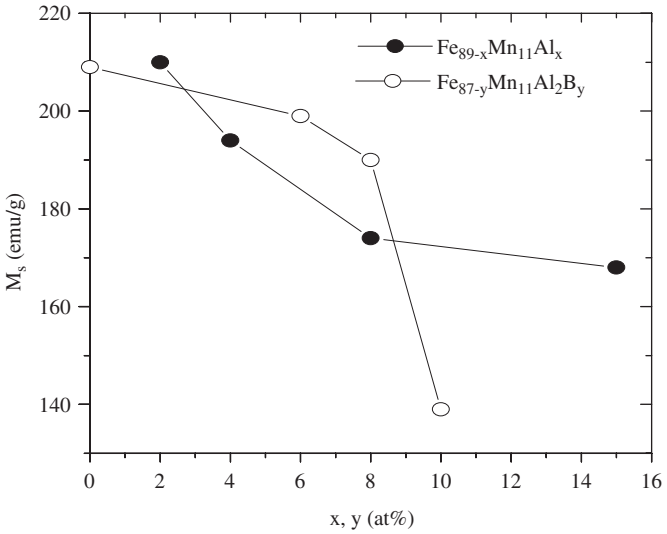

Fig. 2. Saturation magnetization M_s as a function of Al and B content (solid lines are a guide for the eye, only).

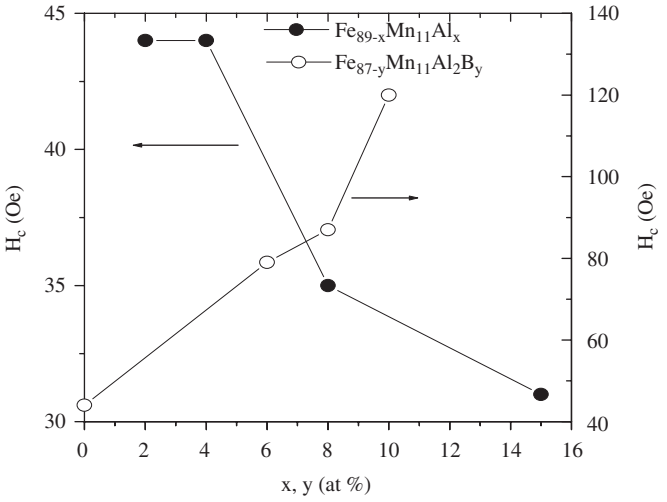

Fig. 3. Intrinsic coercivity H_c as a function of Al and B content (solid lines are a guide for the eye, only).

atoms. For increasing x values ($x = 4$ in Fig. 1b), the same XRD patterns appear, which is indicative of a similar microstructure along the Al variation range. On the other hand, for the B-containing alloys (Fig. 1c), additional peaks at $2\theta = 42.9^\circ$ and 50.9° can be ascribed to the highest (3 2 1) and to (2 1 0) reflections of Fe_3B and Fe_7B, respectively. These additional peaks increase progressively with increasing B concentrations, for which the notably enhanced (1 1 0) refraction peak seems to indicate some texturing for these planes laying orthogonally to the ribbon length.

From $M-H$ curves, the saturation magnetization M_s as a function of Al, B content were determined for both alloy series in Fig. 2. For the original alloy ($x = y = 0$), a rather high M_s value of 210 emu/g is observed (which is close to that of pure iron, $M_s = 218$ emu/g). Further Al additions resulted in progressively decreasing M_s up to $M_s = 168$ emu/g at 15 at% Al. The B-containing alloys displayed a similar reducing monotonous trend for M_s, from 199 emu/g at the initial B concentration to 139 emu/g at $y = 10$.

On the other hand, the intrinsic coercivity H_c as a function of Al and B content is shown in Fig. 3. For the increasing Al alloy series, H_c exhibited initially similar values, followed by a decreasing tendency up to 31 Oe at 15 at% Al. In contrast, H_c showed enhanced values for increasing B concentration, from 44 Oe ($y = 0$) to 120 Oe ($y = 10$).

For the frequency-dependent measurements, Fig. 4 displays the Cole–Cole $\mu_{re}-\mu_{im}$ plots for $Fe_{87}Mn_{11}Al_2$, $Fe_{85}Mn_{11}Al_4$ and $Fe_{81}Mn_{11}Al_2B_6$ alloy samples. For all the compositions, semicircle curves are formed. The alloy relative initial permeability can be determined as the semicircle diameter [4–6]. This permeability decreases slightly from 1375 (at the original $Fe_{87}Mn_{11}Al_2$ composition) to 1185 for 4 at% Al; whereas for the B-containing alloy, a considerable enhanced value of 2063 is observed. In contrast, the relaxation frequency f_x, determined at the maximum of each semicircle (since each μ_{re}, μ_{im} component is a function of frequency) [4–6], showed a remarkable increment from 500 KHz (for $Fe_{87}Mn_{11}Al_2$ alloy) up to 2 MHz (at 4 at% Al) followed by sharp decrease to 170 kHz for the B-containing alloy.

4. Discussion

As it was shown by XRD results, the microstructure of the $Fe_{89-x}Mn_{11}Al_x$ ($x = 2, 4, 8, 15$) alloy series comprises disordered BCC α-Fe phase along the whole Al range composition studied and thus, the reduction in M_s can be attributed to a dilution effect of the unit cell magnetic moment by increasing non-magnetic Al atoms. The concomitant reduction in H_c seems to be a consequence of the microstructure evolution from an irregular dendritic-

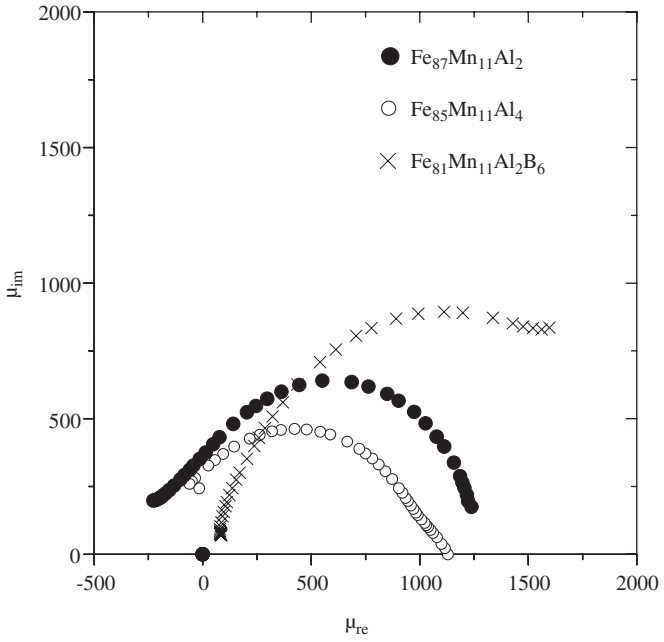

Fig. 4. Cole–Cole plots for selected alloys.

polycrystalline structure (at the initial Al concentrations—up to 4 at%), which favours the pinning of the magnetic domain walls, to an homogeneous polycrystalline distribution, which facilitates the domain wall displacement and thus, a reduced coercivity. In contrast, the increasing coercivity of the B-containing alloy series can be explained in terms of the increasing number of domain wall pinning centres promoted by the precipitation of other phases as the B content rises. Part of this B addition contributes to the dilution of magnetic moment of the unit cell, as it is reflected by the diminished values of M_s.

Within the context of the complex permeability formalism, the observed Cole–Cole $\mu_{re}-\mu_{im}$ plots can be associated to the reversible bulging of the magnetic domain walls and thus, to the alloy initial permeability [4,5]. In addition, the relaxation frequency f_x corresponds to the threshold frequency value at which a relaxation-type dispersion occurs indicating that reversible bulging of domain walls is no longer the active magnetization mechanism. Instead of this, a magnetization process with a lower time constant, namely the spin rotation, remains as active mechanism [4,5]. Usually, the expected semicircles Cole–Cole locus for a relaxation-type dispersion is at the positive $\mu_{re}-\mu_{im}$ axes, in opposition to a natural resonance process, which forms a full circle including negative μ_{re} components [4]. For the B-doped alloy showed in Fig. 4, a clear relaxation dispersion is observed, reflecting the transition from reversible bulging of domain walls to spin rotation. In contrast, the alloys with 2 and 4 at% Al encompasses negative μ_{re} components, which is indicative of a precursor resonance-type process alongside with the relaxation dispersion of the initial permeability [4]. This combined effect is a consequence of intermediate values of the damping factor β reflecting a balance between domain wall inertia and domain wall damping [4]. For the alloy with increasing Al content, the observed reduction in μ_{re} should be attributed to reduced M_s values, while the marked enhancement in f_x can be presumably ascribed to a diminished β value, since $f_x \sim \beta^{-1}$ [7]. For the B containing alloy, the enhanced μ_{re} should be a consequence of a grain size refinement of the polycrystalline distribution present for these ribbons, as it has been reported in similar alloy systems [8].

Although FeMnAl-based alloys have been studied since long ago [1–3], it is worth to mention that, to the authors knowledge, no previous reports neither on *melt spun* FeMnAl alloys nor on the characterization of their magnetization mechanisms had been made. It is significant for instance that, the relaxation frequency of these rapidly solidified FeMnAl alloys could be improved up to 2 MHz, which is comparable to the f_x of some high frequency Ni–Zn, Zn–Mn ferrites ($f_x = 1.0$ MHz and 3.4 MHz, respectively [9,10]) and thus (in addition to their high M_s values) rendering these alloys a suitable material for high frequency technology applications.

5. Conclusions

Magnetic properties of disordered melt spun $Fe_{89-x}Mn_{11}Al_x$ ($x = 2, 4, 8, 15$) and $Fe_{87-y}Mn_{11}Al_2B_y$ ($y = 6, 8, 10$) alloy series were studied by VSM and complex permeability measurements. M_s exhibited an initial high value of 210 emu/g and a decreasing tendency with further Al and B concentration. On the other hand, the initial permeability showed variations within the range 1000–2000 whereas the relaxation frequency displayed a maximum of 2 MHz for Al-containing alloys.

Acknowledgements

The authors are grateful for the helpful technical assistance of G. Lara. One of the authors (F. Nava) acknowledges the scholarship given by COSNET.

References

[1] J. Restrepo, G.A. Perez Alcazar, J.M. Gonzalez, Hyperfine Inter. 134 (2001) 27.
[2] C. Gonzalez, G.A. Perez Alcazar, L.E. Zamora, J.A. Tabares, J.M. Greneche, J. Phys.: Condens. Matter 14 (2002) 6531.
[3] H. Bremers, J. Hesse, H. Ahlers, J. Sievert, D. Zachmann, J. Alloys Compd. 366 (2004) 67.
[4] R. Valenzuela, H. Montiel, M.P. Gutierrez, I. Betancourt, J. Magn. Magn. Mater. 294 (2005) 239.
[5] R. Valenzuela, Phys. B 299 (2001) 280.
[6] P. Quintana, E. Amano, C. Echavarrieta, R. Valenzuela, N. Murillo, J.M. Blanco, J. Gonzalez, J. Magn. Magn. Mater. 160 (1996) 245.
[7] K.L. Garcia, R. Valenzuela, IEEE Trans. Magn. 34 (1998) 1162.
[8] M.M. Rico, J.M. Greneche, G.A. Perez Alcazar, J. Alloys Compd. 398 (2005) 26.
[9] J.T.S. Irving, A.R. West, E. Amano, A. Huanosta, R. Valenzuela, Solid State Ionics 40/41 (1990) 220.
[10] E. Carrasco, K.L. Garcia, R. Valenzuela, IEEE Trans. Magn. 34 (1998) 1159.